Original Article

A Nanocomposite Shield Constructed for Protection Against the Harmful Effects of Dental X-Rays

Simel Ayyıldız[1], Elif Hilal Soylu[2], Jülide Özen[3], Semra İde[4], Kıvanç Kamburoğlu[5]✉

[1]Associate Professor, Department of Prosthodontics, Dental Health Sciences Center, Gülhane Military Medical Academy, Ankara, Turkey
[2]Engineer, Department of Physics, Karadeniz Technical University, Faculty of Science and Literature, Trabzon, Turkey
[3]Associate Professor, Private Practitioner, Ankara, Turkey
[4]Professor, Department of Physics Engineering, Faculty of Engineering, Hacettepe University, Ankara, Turkey
[5]Associate Professor, Department of Dentomaxillofacial Radiology, Faculty of Dentistry, Ankara University, Ankara, Turkey

Abstract
Objectives: This study aimed to compare a number of new nano-composites capable of protecting the jaw from ionizing radiation.
Materials and Methods: Four different types of nano-powders [Ti, Zr (IV) oxide, Ag and Co] were mixed in a polymer matrix to create nano-composites with doping values of 8% in weight. Small-angle X-ray scattering (SAXS) analysis was performed using a HECUS-SAXS system with 50 kV- 50 mA. Co nano-composites (Co-pnm) yielded the most promising values of the four nanocomposites tested in terms of X-ray absorption. Thus, 4×2 cm Co-pnm samples of different thicknesses (0.20, 0.50, 0.57 and 0.60 cm) were prepared, and SAXS analysis was performed in order to assess the effects of material thickness on x-ray absorption. An experimental multi part shield was constructed from Co-pnm around tooth #36 to test the effect of nanomaterial on the image quality under X-ray beam.
Results: Logarithmic distributions of the transmitted intensity values (I) showed that 0.20 cm Co-pnm had the highest transmission value (16.05) followed by 0.50 cm Co-pnm (15.44), 0.57 cm Co-pnm (15.07) and 0.60 cm Co-pnm (15.06). The 0.2 cm Co-pnm had an effective radius of the nano-aggregation value (77.44 Å) lower than that of the other thicknesses (0.50, 0.57 and 0.60 cm) of Co-pnm, which had similar values ranging from 66.22 to 66.34 Å. The 0.50 cm Co-pnm had the lowest D_{max} value of the different thicknesses of Co-pnm tested.
Conclusion: Co nanocomposite can be used as a protection shield for the harmful effects of dental X-ray.
Keywords: Mutagenicity Tests; Radiography; Diagnostic; Nanocomposites; Polymer; Matrix

✉ Corresponding author:
K. Kamburoğlu, Department of Dentomaxillofacial Radiology, Faculty of Dentistry, Ankara University, Ankara, Turkey

Dtkivo@yahoo.com

Received: 22 June 2014
Accepted: 20 January 2015

Journal of Dentistry, Tehran University of Medical Sciences, Tehran, Iran (2015; Vol. 12, No. 5)

INTRODUCTION

Ionizing radiation can produce detrimental changes in several classes of macromolecules found in cells [1]. It also causes damage to deoxyribonucleic acid (DNA) and DNA-protein cross-links and induces cellular death

[2]. There is a direct relationship between the effects of ionizing radiation and the type of tissue receiving the radiation and the absorbed radiation dose. Dental radiology represents the most frequently applied radiological diagnostic tool, the enormous diagnostic benefits of which make its use indispensable. However, while individual doses and risks are low, the collective dose is not inconsiderable [3,4].

Patients most commonly receive ionizing radiation to the head, and several studies have shown dental radiography to be associated with an increased risk of meningioma, brain cancer and parotid gland tumors as well as breast cancer [5-9]. Four different types of x-ray examination techniques are commonly used in dentistry for diagnostic purposes: posterior bitewings, periapical films, lateral cephalometric radiographs and panoramic radiographs (OPG). In addition, cone-beam computerized tomography (CBCT) has recently been accepted as an emerging x-ray technology in dentomaxillofacial imaging [10,11]. All these imaging techniques have been implicated in nuclear alterations of stomatognathic system cells that are closely related to genotoxicity. The fact that imaging may subject regions not specifically under consideration to x-ray radiation [2,12,13] warrants an assessment of what types of protective devices can be produced from nano-materials to shield areas of the jaw and the rest of the body outside the area of interest from the harmful effects of x-rays.

Many techniques are available for evaluating the structural characteristics of materials that have metallic particles. Small angle X-ray scattering is one such technique used for the structural characterization of solid and fluid materials in the nanometer (nm) range. Measurements are commonly performed in transmission geometry by using a narrow, well-collimated and intense X-ray beam. X-ray absorption is related to the thickness of the material and the atomic numbers of the elements from which it is composed.

A narrow beam of mono-energetic photons with an incident intensity of I_o will have a transmitted intensity of I that can be calculated using the equation; $I/I_o = \exp[-(\mu/\rho)\,x]$ (eq 1), where x represents the mass thickness (the mass per unit area) and ρ represents the density of the material through which the ray passes. Mass thickness can also be calculated by multiplying the thickness (t) by the density (ρ) as $x = \rho t$, allowing eq1 to be rewritten as $\ln I = \ln I_o - \mu t$ (eq 2). Once I_o, I and t values have been established, the linear attenuation coefficient of μ can be established from the slope of [ln I - t] [14]. For the evaluation of SAXS data, GNOM [15] and DAMMIN [16] computer programs are used. GNOM is an indirect transform program for small-angle scattering data processing that reads one-dimensional scattering curves (possibly smeared with instrumental distortions) and evaluates a distance distribution function p for monodispersal systems or a size distribution function D for polydispersal systems. GNOM creates the function D_{max} (indicates the nanostructures' maximum overall size and can be determined using pair distance distributions of the nano-aggregates) and the input file required for *ab-initio* modeling [15].

DAMMIN uses small angle x-ray scattering to recreate *ab-initio* low-resolution shapes of randomly oriented particles in solution (e.g., biological macromolecules) [16]. Therefore, this study aimed to synthesize and compare a number of new nano-composites capable of protecting the jaw and the rest of the body from the harmful effects of ionizing radiation by absorbing x-rays with SAXS analyzing method and to test the availability of designing an intraoral shield and its affect on the image quality of periapical radiography using the most promising nanocomposite (Co).

MATERIALS AND METHODS

Synthesis of nano-composites:

Four different types of nano-powders [Ti, Zr (IV), Ag and Co] ranging in size from 5-70 nm

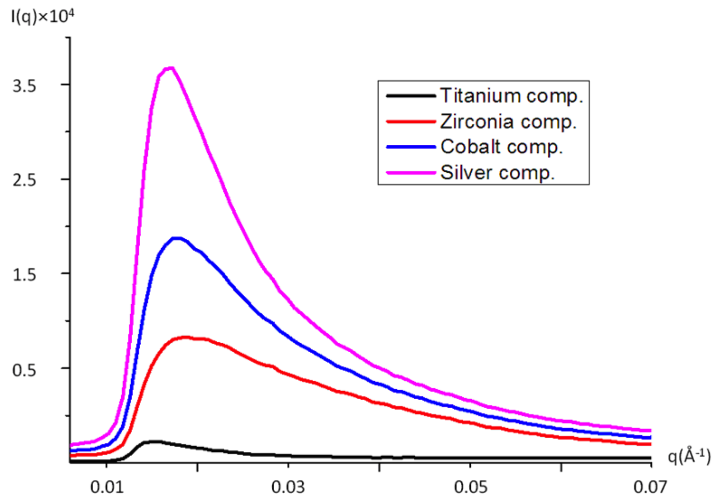

Fig. 1. SAXS profiles of polymer-based Ag, Co, Zr and Ti nano-composites (0.50 cm thick) measured according to q (magnitude of transmitted scattering vector).

were obtained from chemical manufacturers [Sigma Aldrich (578347-10G, 544760-25G); Alfa Aesar (231-158-0, 232-033-3)] and were mixed in a polymer matrix to create nanocomposites with doping values of 8% in weight, without any additional purification. The matrix was prepared using self-cure acrylic resin powder (Akribel, Self Curing Denture Acrylic Powder, Atlas-Enta A.Ş., Izmir, Turkey) and heat-cure acrylic liquid (Paladent 20, Heraeus, Kulzer, Hanau, Germany) according to the manufacturers' instructions. Each mixture was poured into a cylindrical plastic mold and polymerized with a special heat-pressure polymerization device (Ivomat IP3, Ivoclar Vivadent AG, Schaan, Lichtenstein) under 6-bar pressure at 40^0C for 15 minutes. The composite cylinders were then processed and shaped in rectangular form with 4×2 mm dimensions and 0.50 cm thickness, using a high-speed dental hand piece (K5Plus, Kavo, Biberach, Germany). A 320-grit SiC sandpaper (Norton, Worchester, MA, USA) was used for the surface correction of the samples and polishing procedures were applied with pumice paste.

SAXS analysis:

SAXS measurement was performed using HECUS-SAXS system with 50 kV- 50 mA, CuK_α (λ=1.54 Å) radiation line collimation and position sensitive detectors (~54 μm resolution, 1024 channels). SAXS patterns for the nanocomposites are shown in Fig. 1. Effective radius of the nano-aggregations, forms, most probable *ab-initio* shape and pair-distance distributions of the samples were obtained through analyses of the experimental data. SAXS data were evaluated using GNOM and DAMMIN software programs.

X-ray absorbance calculation of the synthesized nano-composites:

The x-ray absorbance values of the nano-composites were calculated using the eq 1 ($I/I_0=\exp[-(\mu/\rho)\,x]$) and eq2 ($\ln I = \ln I_o - \mu t$). Ti nano-composites (Ti-pnm) yielded the most promising values of the four nano-composites tested in terms of x-ray absorption followed by Co nano-composites (Co-pnm) and Ti-pnm (Fig. 2).

In this study, Co-pnm samples of different thicknesses (0.20, 0.50, 0.57 and 0.60 cm) were

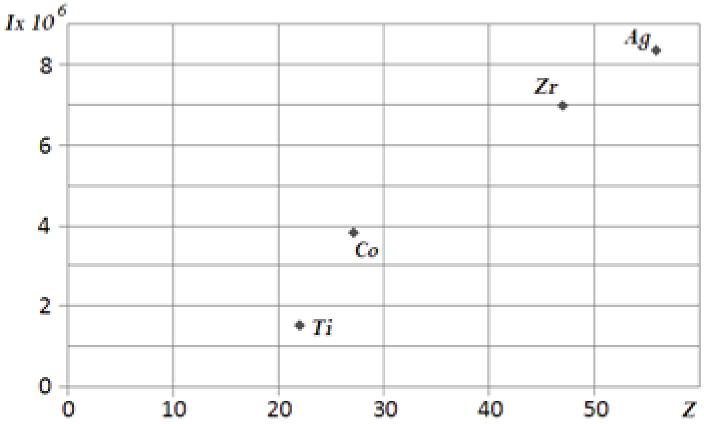

Fig. 2. Nanoparticle atomic number (Z); the differences in total transmitted intensities (I) of nano-composites.

prepared, and SAXS analysis was performed in order to assess the effects of material thickness on x-ray absorption. Prior to SAXS testing, sample thickness was confirmed using a digital caliper (Tresna, Guanglu Europa GmbH, Essen, Germany).

Preparation of experimental shield:

An experimental shield was constructed from Co-pnm to act as an x-ray protector for the human mandible surrounding tooth #36 (Fig. 3a, b). Two layers of pink wax were adapted over teeth #35, 36 and 37, and the acrylic resin-based mass was adapted directly over the wax.

The resin mass was shaped with the aid of a spatula, and the polymerization procedure was completed using a heat-polymerization device.

Surface correction was performed using laboratory hand-pieces to obtain a uniform thickness of 0.50cm, as measured by a digital caliper.

The prepared matrix was then cut into three pieces, two of which were shortened to provide a clear view of the mesial and distal parts of tooth #36.

The remaining part was adapted to fit over tooth #36 and the two other parts of the shield to create an easily adaptable, multi-unit stent (Fig. 3a, b).

Intraoral radiographs were taken with the shield in place (Fig. 3c).

RESULTS

Absorbance

SAXS profiles calculated using the magnitude of the transmitted scattering vector showed Ti to have the highest absorbance value, followed by Zr, Co and Ag, respectively (Fig. 1).

Nanocomposite x-ray transmittance values (Ix10^6) are shown in Fig. 2. As the figure shows, Ti had the lowest transmittance value, followed by Zr.

Table 1. Experimental results about the X-ray absorbance of cobalt nanocomposite

Transmitted Int. (I × 10^6)	**Layer Thickness t (cm)**	***ln I***	I_o	μ (cm^{-1})
9.389	0.20	16.05	*ln* I_o = 16.6 *(graphic)*	2.51±0.06
5.024	0.50	15.44		
3.521	0.57	15.07	I_o=16.2x10^6	(Slope of the graphic)
3.462	0.60	15.06		

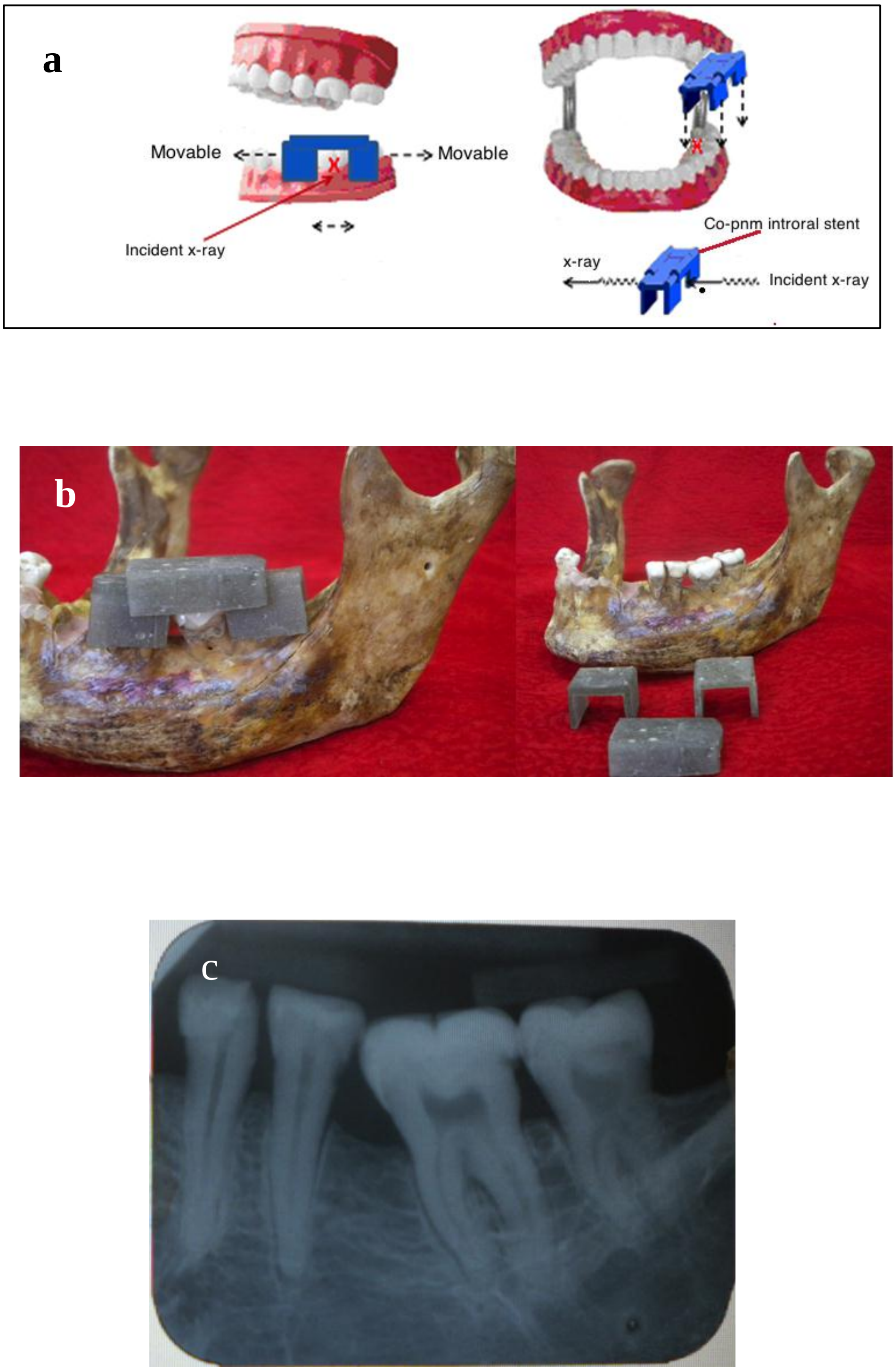

Fig. 3. Schematic view and photograph of the intraoral experimental shield (a,b). Periapical image of the shield (c).

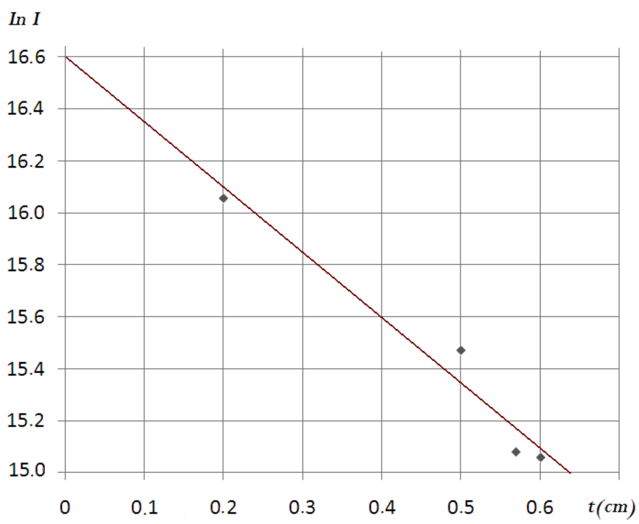

Fig. 4. Logarithmic transmitted intensity as a function of thickness for Co nanocomposite.

These findings indicate that Ti absorbs the majority of transmitted x-rays, whereas Ag scatters the x-rays.

Linear absorption coefficients of the different thicknesses of Co-pnm (Fig. 4) were calculated according to eq 1 using the I, I_o and μ values given in Table 1. Logarithmic distributions of the transmitted intensity values (I) showed that 0.20 cm Co-pnm had the highest transmission value (16.05) followed by 0.50 cm Co-pnm (15.44), 0.57 cm Co-pnm (15.07) and 0.60 cm Co-pnm (15.06). Thus, the absorbance values were as follows: 0.60>0.57> 0.50>0.20 cm Co-pnm.

SAXS results:

Figures 5 and 6 show, respectively, the graphs of the effective radius of the nano-aggregation values and the D_{max} values for Co-pnm of different thicknesses. As seen in Fig. 5, the 0.2 cm Co-pnm had an effective radius of the nano-aggregation value (77.44 Å) higher than that of the other thicknesses (0.50, 0.57 and 0.60 cm) of Co-pnm, which had similar values ranging from 66.22-66.34Å. As seen in Fig. 6, the 0.20 cm Co-pnm had the highest D_{max} value of the different thicknesses of Co-pnm tested.

X-ray analysis of shield:

Standard periapical x-ray radiograph showed that the Co-pnm stent appeared as a radiopacity over the occlusal surface of the teeth and did not affect subjective image quality.

DISCUSSION

X-rays have been widely used for decades as diagnostic tools in the field of dentistry. Studies have clearly shown that ionizing radiation induces cellular death by karyorrhexis, pyknosis and karyolysis. Individuals continually exposed to X-rays (for endodontic, orthodontic, implant and other purposes) may later develop cancer as a result of genotoxic/cytotoxic cell differentiation [17,18]. The literature contains insufficient information regarding the use of nano-materials in providing regional protection from the harmful effects of X-rays on areas of the body and jaw outside the area of consideration. In the field of nanotechnology, both small- and wide-angle x-ray scattering methods have been effectively used to study polymer matrix-based nano-composites [19]. The present study used Ti, Zr, Co and Ag nanoparticles in the synthesis of nano-composites.

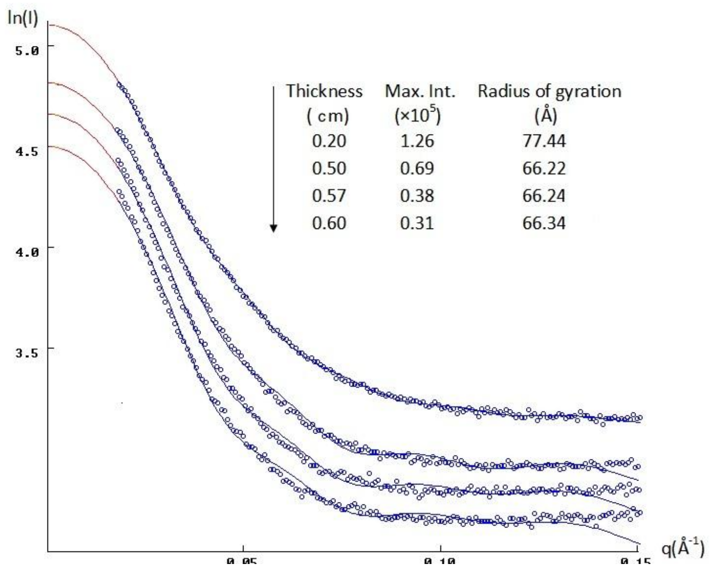

Fig. 5. SAXS patterns (blue circles) and *ab-initio* fitting scatter curves of Co nano-composites of different thicknesses.

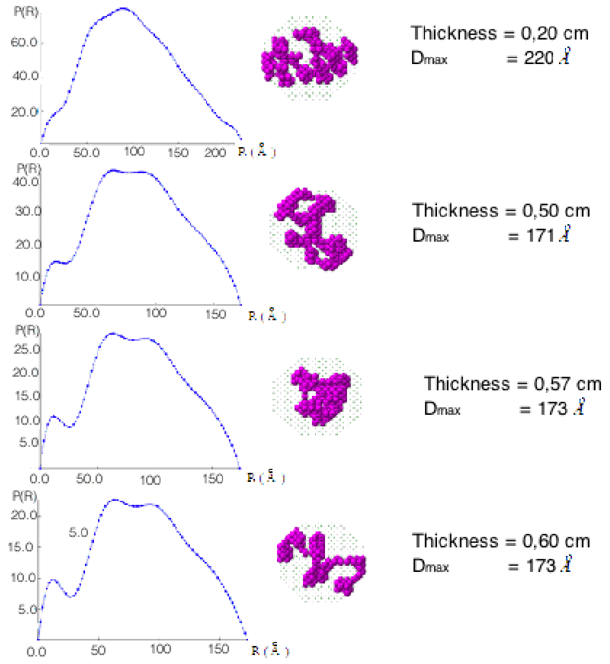

Fig. 6. Pair-distance distributions and most probable shapes of the sample nano-aggregates.

Co, Ag and Ti are transition metals that do not form binary phases in polymeric media and demonstrate negligible solubility.

Zirconia is a white amorphous powder that shows a homogeneous distribution in a composite matrix.

Zirconium (Zr) and Ti are widely used in dentistry for rehabilitation. The brittleness of these nanoparticles makes them easy to synthesize. Other materials with high mass attenuation coefficients, such as lead (Pb), are also widely used to protect biological tissue from the harmful effects of high energy x-rays for many years [23-25]. Pb and Co have Mohs hardness values of 1.5 and 5.0, respectively. The low brittleness, hardness and oxidation characteristics of Pb make it very difficult to synthesize nanoparticles from this element. The main reason of using nanoparticles in this study was their low weight in any composite material [25]. Thus, Ti, Zr, Co and Ag have low weights as in nano-powder form and the materials that will be produced from these materials will not be affected by the nanoparticles of metallic alloys. However, the traditional x-ray protectors that contain Pb are very heavy for use [23-26]. As Fig. 1 shows, Ti and Zr matrixes had lower x-ray scattering angle to transmitted scattering vector ratios than the Co and Ag matrixes of similar thicknesses. However, as Fig. 2 shows, the total transmitted intensities of the nanocomposite matrixes varied in line with their atomic numbers of their constituent nano-composites, so that the Ti matrix had the lowest total transmitted intensity, followed by the Co matrix. The SAXS analysis conducted in this study found Ti to have the best x-ray absorption values; however, due to the high cost of obtaining Ti nano-powder, detailed examinations were conducted using the nanocomposite containing Co, which was also found to have adequate protective properties.

GNOM [15] and DAMMIN [16] software analyses used to evaluate the findings of SAXS showed that the tested 0.6 cm thick Co-pnm sample absorbed the greatest amount of x-ray radiation (Figs. 4-5) or transmitted the lowest x-ray radiation. However, although the maximum absorbance was found for 0.6 cm thickness, 0.5 cm thickness was chosen because in this thickness, the shapes, pair distance distributions and numbers of the nano-aggregations, and surface morphology of the plate are well optimized to cause bigger absorbance. Thus, the experimental intraoral shield was constructed from 0.5 cm thickness. The weight of the protective shield did not increase with an increase in the thickness. With the advances in technology, economical and disposable materials that contain Co nano-powder may be produced to protect the health of patients.

In this study, an experimental intraoral Co-pnm shield was constructed and tested over a human mandible to check the formability of resin matrix after the addition of metallic nano-powder. Although the shield appeared as a radiopacity over the occlusal surface of the teeth, this did not affect the visibility of periapical or surrounding tissue. Similar shields may be constructed specifically for other parts of the stomatognathic system or any part of the body using Co or other nano-powders and may be used for a variety of diagnostic and/or treatment purposes. As the technology advances, shields may be fabricated in thin-film coating, in rubber-dam like form or in plastic mouth guard form, in the future. The main limitation of this study was the preliminary design of the shield. The Co-pnm shield was fabricated only to observe the manipulative property of the acrylic resin and any effect on the diagnosis made based on periapical intraoral films. It was designed over a human mandible that has surrounding soft tissue of the stomatognathic system. Animal studies may be performed to mimic the clinical conditions.

CONCLUSION

In conclusion, the Co nanocomposite fabricated in this study was found to have a linear absorption coefficient value (μ) of 2.51 ± 0.06 cm^{-1}, indicating that it may be used as a shield material to protect against the harmful effects of x-rays during diagnosis and dental rehabilitation. Moreover, the Co nanocomposite was found to have an effective radius of the nano-aggregation ranging from 66.22 to 77.94 Å, demonstrating a uniform distribution that can be adequately controlled. In light of these findings, further studies may be undertaken to examine new applications for cobalt nanocomposite in dentomaxillofacial radiology and radiotherapy.

REFERENCES

1- Angelieri F, Carlin V, Saez DM, Pozzi R, Riberio DA. Mutagenicity and cytotoxicity assessment in patients undergoing orthodontic radiographs. Dentomaxillofac Radiol. 2010 Oct;39(7):437-40.

2- Ribeiro DA. Cytogenetic biomonitoring in oral mucosa cells following dental X-ray. Dentomaxillofac Radiol. 2012 Mar;41(3):181-4.

3- Horner K. Review article: radiation protection in dental radiology. Br J Radiol. 1994 Nov;67(803):1041-9.

4- Boraks G, Tampelini FS, Pereira KF, Chopard RP. Effect of ionizing radiation on rat parotid gland. Braz Dent J. 2008;19(1):73-6.

5- Walker C, van der Putten W. Patient dosimetry and a novel approach to establishing diagnostic reference levels in dental radiology. Phys Med. 2012 Jan;28(1):7-12.

6- Abt E. Can dental x-rays increase the risk of meningioma? Evid Based Dent. 2012 Jun;13(2):37-8.

7- Memon A, Godward S, Williams D, Siddique I, Al-Saleh K. Dental x-rays and the risk of thyroid cancer: A case-control study. Acta Oncol. 2010 May;49(4):447-53.

8- Ma H, Hill CK, Bernstein L, Ursin G. Low-dose medical radiation exposure and brest cancer risk in women under age 50 years overall and by estrogen and progestron receptor ststus: Results from a case control and a case-case comparision. Breast Cancer Res Treat. 2008 May;109(1):77-90.

9- Preston-Martin S, White SC. Brain and salivary gland tumors related to prior dental radiography: Implications for current practice. J Am Dent Assoc. 1990 Feb;120(2):151-8.

10- Longstreth WT, Phillips LE, Drangsholt M, Koepsell TD, Custer BS, Gehrels JA, et al. Dental x-rays and the risk of intracranial meningioma. A population-based case-control study. Cancer. 2004 Mar 1;100(5):1026-34.

11- Wright B. Contemporary medic-legal dental radiology. Aust Dent J. 2012 Mar;57 Suppl 1:9-15.

12- Ribeiro DA, Sannomiya EK, Pozzi R, Miranda SR, Angelieri F. Cellular death but not genetic damage in oral mucosa cells after exposure to digital lateral radiography. Clin Oral Investig. 2011 Jun;15(3):357-60.

13- El-Ashiry EA, Abo-Hager EA, Gawish AS. Genotoxic effects of dental panoramic radiography in children. J Clin Pediatr Dent. 2010 Fall;35(1):69-74.

14- Ladd MFC, Palmer RA. Structure determination by X-ray Crystallography 2nd Ed. New York and London: Plenum Press; 1988, Appendix A4, p.423.

15- Svergun DI. Determination of the regularization parameter in indirect-transform methods using perceptual criteria. J Applied Crystallography 1992;25:495-503.

16- Svergun DI. Restoring low resolution structure of biological macromolecules from solution scattering using simulated annealing. Biophys J. 1999 Jun;76(6):2879-86.

17- Riberio DA, de Oliveira G, de Castro G, Angelieri F. Cytogenetic biomonitoring in patients exposed to dental X-rays: comparison between adults and children. Dentomaxillofac Radiol. 2008 Oct;37(7):404-7.

18- Cerqueira EM, Meireles JR, Lopes MA, Junqueira VC, Gomes-Filho IS, Trindade S, et al. Genotoxic effects of X-rays on keratinized mucosa cells during panoramic dental radiography. Dentomaxillofac Radiol. 2008 Oct;37(7):398-403.

19- Paul DR, Robeson LM. Polymer nanotechnology: Nanocomposites. Polymer 2008; 49 : 3187-3204.

20- Loizou E, Butler P, Porcar L, Kesselman E, Talmon Y, Dundigalla A, et al. Large scale structures in nanocomposite hydrogels.

Macromolecules 2005; 38: 2047-9.

21- Schmidt G, Nakatani AI, Butler PD, Karim A, Han CC. Shear orientation of viscoelastic polymer-clay solutions probed by flow birefringence and SANS. Macromolecules 2000; 33: 7219-22.

22- Schmidt G, Nakatani AI, Han CC. Rheology and flow-birefringence from viscoelastic polymer-clay solutions. Rheol Acta 2002; 41: 45-54.

23- Greenwood JN. The refining and physical properties of lead. Metal Rev 1961;74:279-352.

24- Nambiar S, Osei EK, Yeow JTW. Polymer nanocomposite-based shielding against diagnostic X-rays, J Appl Polym Sci 2013; 127: 4939-46.

25- Lisiecki I, Pileni MP. Synthesis of well-defined and low size distribution cobalt nanocrystals: The limited influence of reverse micelles. Langmuir 2003, 19(22), 9486-9489.

26- Lisiecki I, Pileni MP. Synthesis of well defined and low size distribution cobalt nanocrystals: The limited influence of reverse micelles, Langmuir 2003; 19:9486-89.